

Supplemental Information.

Figure S1 related to main text and Experimental Procedures.

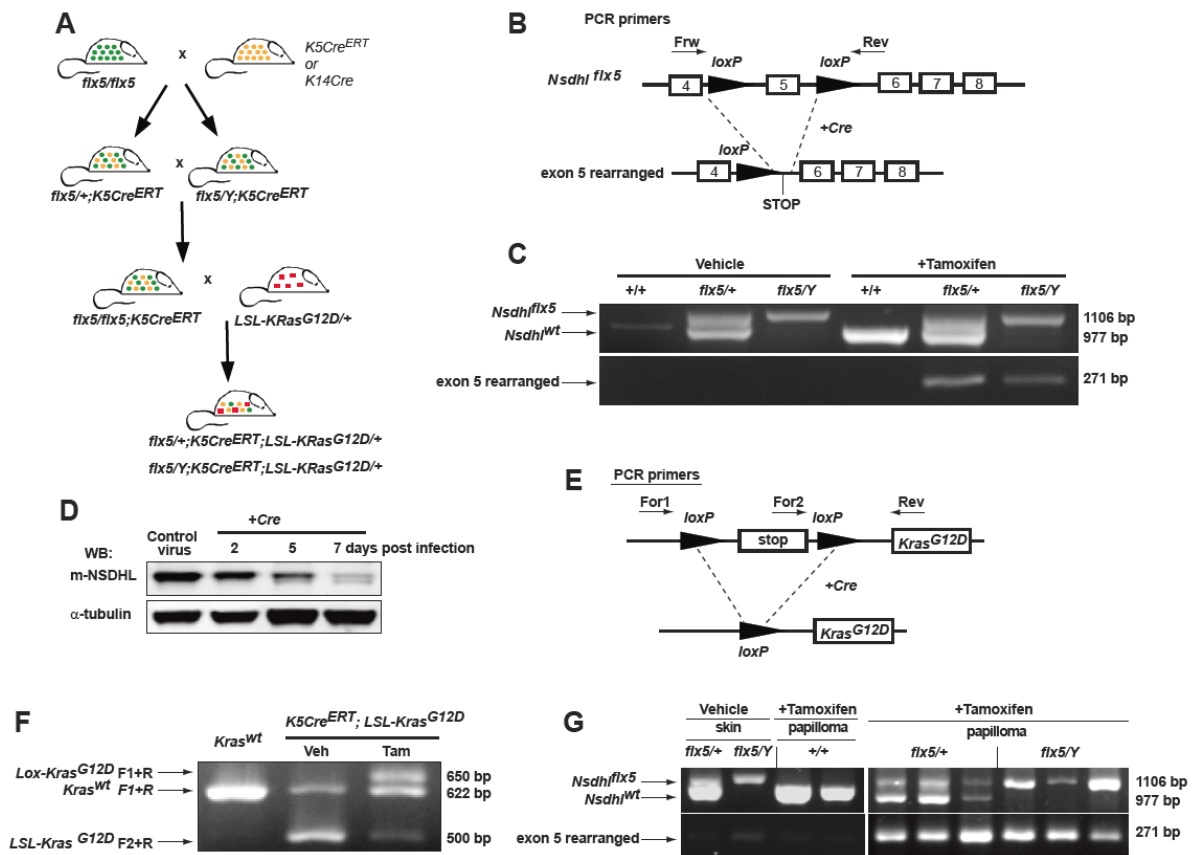


Figure S1. Conditional *Nsdhl* knockout and Cre-activated *KRas^{G12D}* mouse models. **(A)** Breeding scheme. The *Nsdhl^{flx5/flx5}* females (shown as *flx5/flx5*) were crossed with Tg(Krt5-Cre/ERT2)Ajdg (shown as *K5Cre^{ERT}*) males. Their progeny were used for the next breeding to obtain the *Nsdhl^{flx5/flx5}* females carrying a *K5Cre^{ERT}* allele. These *K5Cre^{ERT};Nsdhl^{flx5/flx5}* females were further crossed to heterozygous *LSL-Kras^{G12D/+}* males to generate *K5Cre^{ERT};LSL-Kras^{G12D/+};Nsdhl^{flx5/+}* females and *K5Cre^{ERT};LSL-Kras^{G12D/+};Nsdhl^{flx5/Y}* males that were used to induce papilloma formation. **(B)** Schema of *Nsdhl^{flx5}* rearrangement. 'Frw' and 'Rev' indicate forward and reverse PCR primers, respectively. The knockout allele of *Nsdhl^{flx5}* (Cunningham et al., 2015) contains two *loxP* sites flanking exon 5. Recombination of these sites mediated by a

transgenic Cre-recombinase leads to removal of the intervening sequence (Liu et al., 1999). **(C)** Agarose gel electrophoresis of PCR products shows appearance of the shortened exon 5 of *Nsdhl* in mice treated with tamoxifen. DNA was isolated from skin snippets 1 month after treatment. **(D)** Western blot analysis of NSDHL protein in *Nsdhl*^{flx5/Y} mouse embryonic fibroblasts treated with Cre-retrovirus. **(E)** Schema of *LSL-Kras*^{G12D} rearrangement (Jackson et al., 2001). **(F)** Agarose gel electrophoresis of PCR products shows appearance of activated *Lox-Kras*^{G12D} transgene in mouse skin as the result of tamoxifen-induced Cre-mediated rearrangement. Mice were treated with tamoxifen (40 mg/ml) or vehicle (Corn oil) for 5 consequent days. The band of 650 bp (*Lox-Kras*^{G12D}) indicates rearranged activated *Kras*^{G12D} transgene. **(G)** Conditional knockout of *Nsdhl*^{flx5} in the skin and in KRAS-induced skin tumors. Mice carrying *Nsdhl*^{flx5}, *LSL-Kras*^{G12D} and *K5Cre*^{ERT} genes were treated with tamoxifen or vehicle. DNA was isolated from skin tumors and skin samples.

Figure S2 related to Figure 1 and 3.

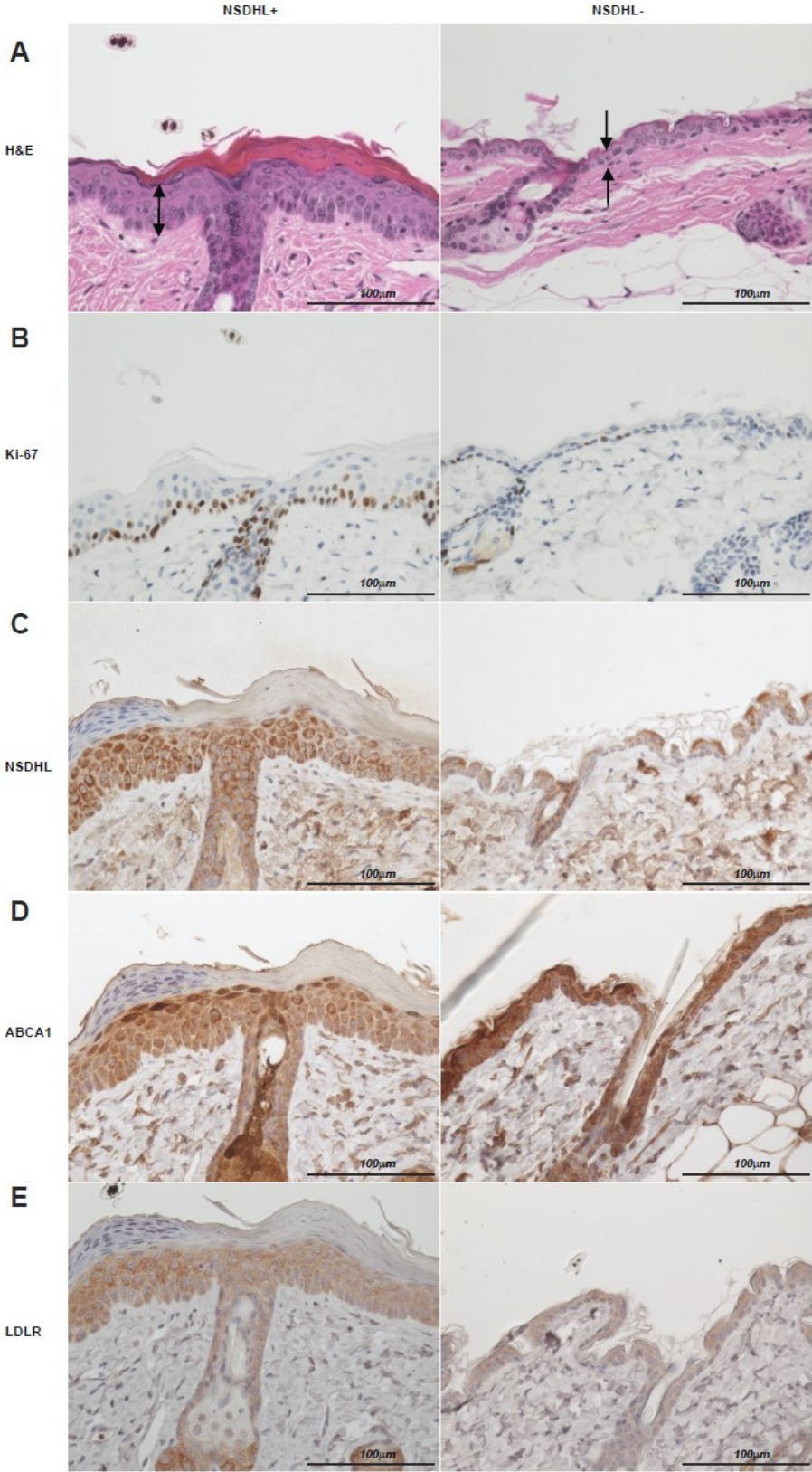


Figure S2. Immunohistochemical staining of NSDHL-deficient areas of the skin in 4 week-old *K14Cre;Nsdhl^{flx5/+}* females; magnification x40. **(A)** Thickness of the basal layer keratinocytes (arrows, H&E staining). **(B)** Reduction of proliferating basal layer keratinocytes (Ki67-positive cells). **(C)** Loss of NSDHL expression. **(D)** Increased level of ABCA1 expression in the NSDHL-null areas. **(E)** Reduced level of LDLR expression in NSDHL-null patches.

Figure S3 related to Figure 1.

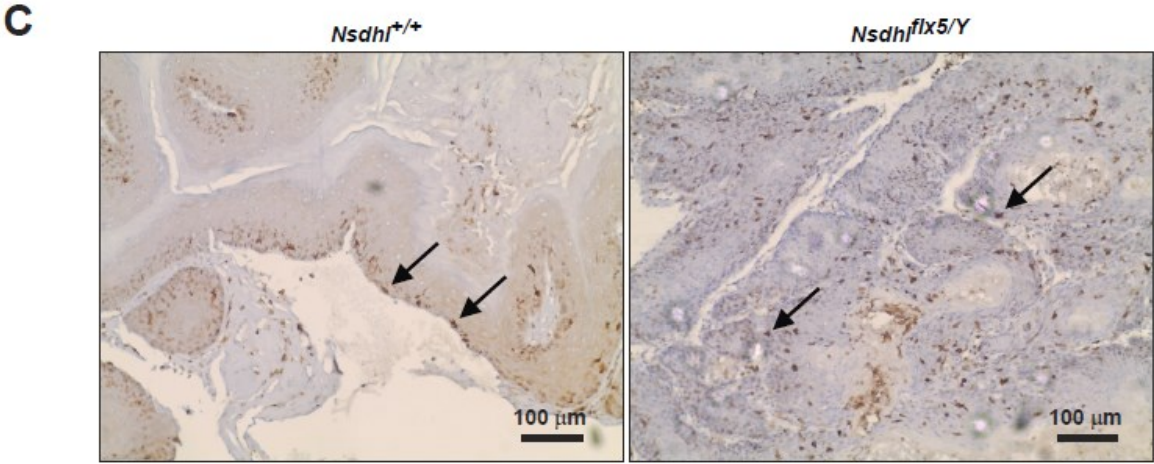
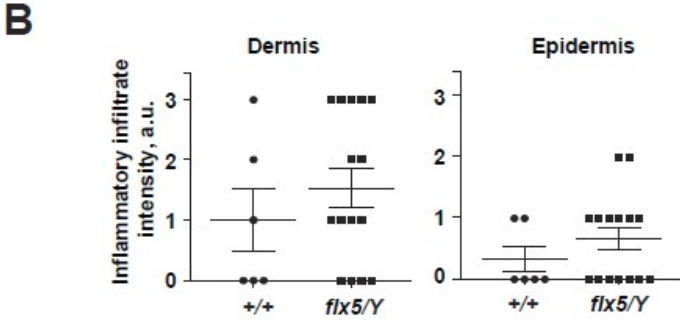
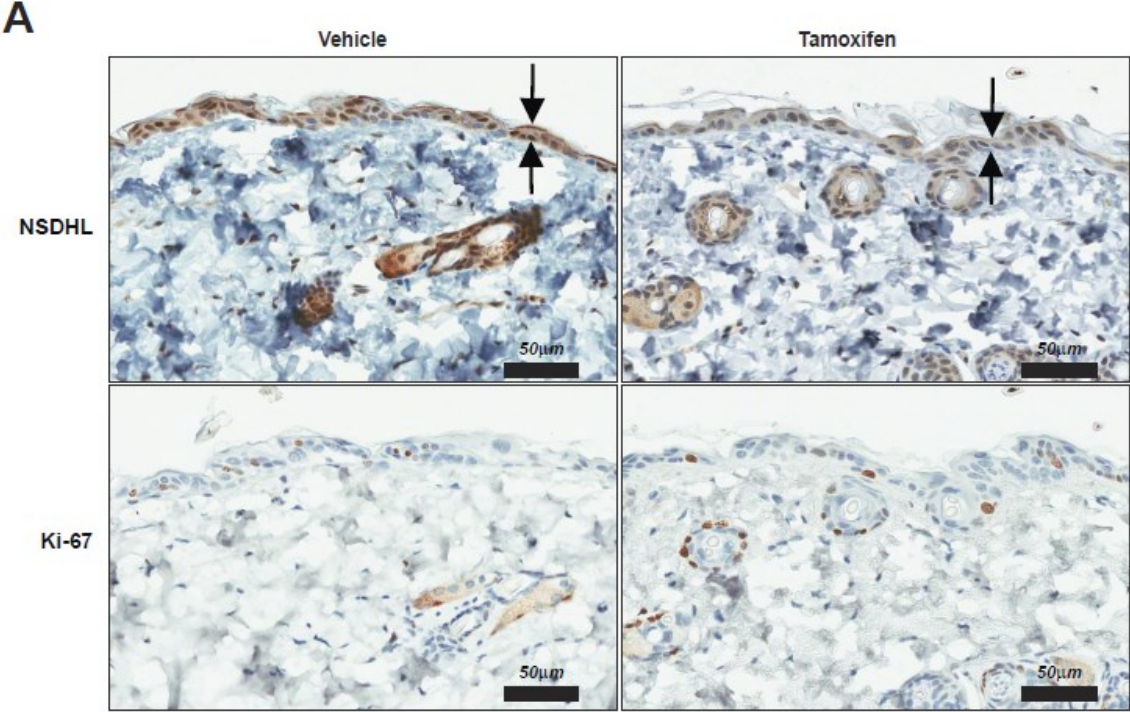


Figure S3. Immunohistochemical staining of NSDHL-deficient skin and papilloma samples. **(A)** Immunohistochemical staining of NSDHL-deficient areas of the skin in tamoxifen-treated adult (14 week-old) $K5Cre^{ERT};Nsdhl^{flx5/Y}$ mice (magnification x40). Loss of NSDHL expression produces no difference in the thickness of the basal layer keratinocytes (top row, arrows) or in the prevalence of proliferating basal layer keratinocytes (bottom row, Ki67-positive cells). **(B)** Inflammatory cellular infiltrates are detectable in skin tumors in dermal and epidermal layers of NSDHL-sufficient ($Nsdhl^{+/+}$) or NSDHL-deficient areas ($Nsdhl^{flx5/Y}$), $p=0.4$. Level of inflammation is scored as 0, 1+, 2+ or 3+. **(C)** Detectable CD3-positive T cells in the dermis of *Kras*-induced skin tumors (magnification x20).

Figure S4 related to Figure 2.

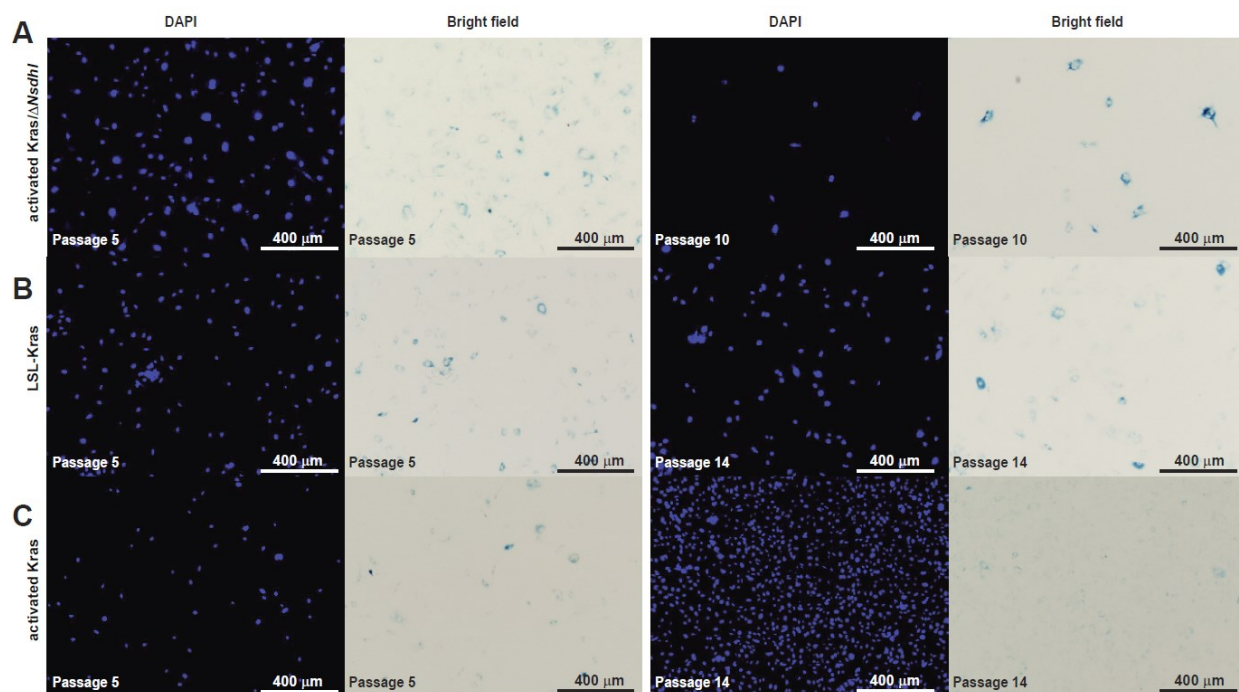


Figure S4. SA-β-galactosidase staining of mouse embryonic fibroblasts at indicated passages; *DAPI*, cell nuclei; *Bright field*, blue cells are SA-β-galactosidase positive: **(A)** activated

Kras^{G12D}/Δ*Nsdhl* fibroblasts following treatment with adeno-Cre (see also Fig. 2D); **(B)** *LSL-KRas*^{G12D} treated with control GFP-expressing adenovirus, inactive *Kras*^{G12D} transgene, intact *Nsdhl*; **(C)** activated *Kras*^{G12D} in *LSL-KRas*^{G12D} treated with adeno-Cre, intact *Nsdhl*;
(magnification x4)

Figure S5 related to Figure 5.

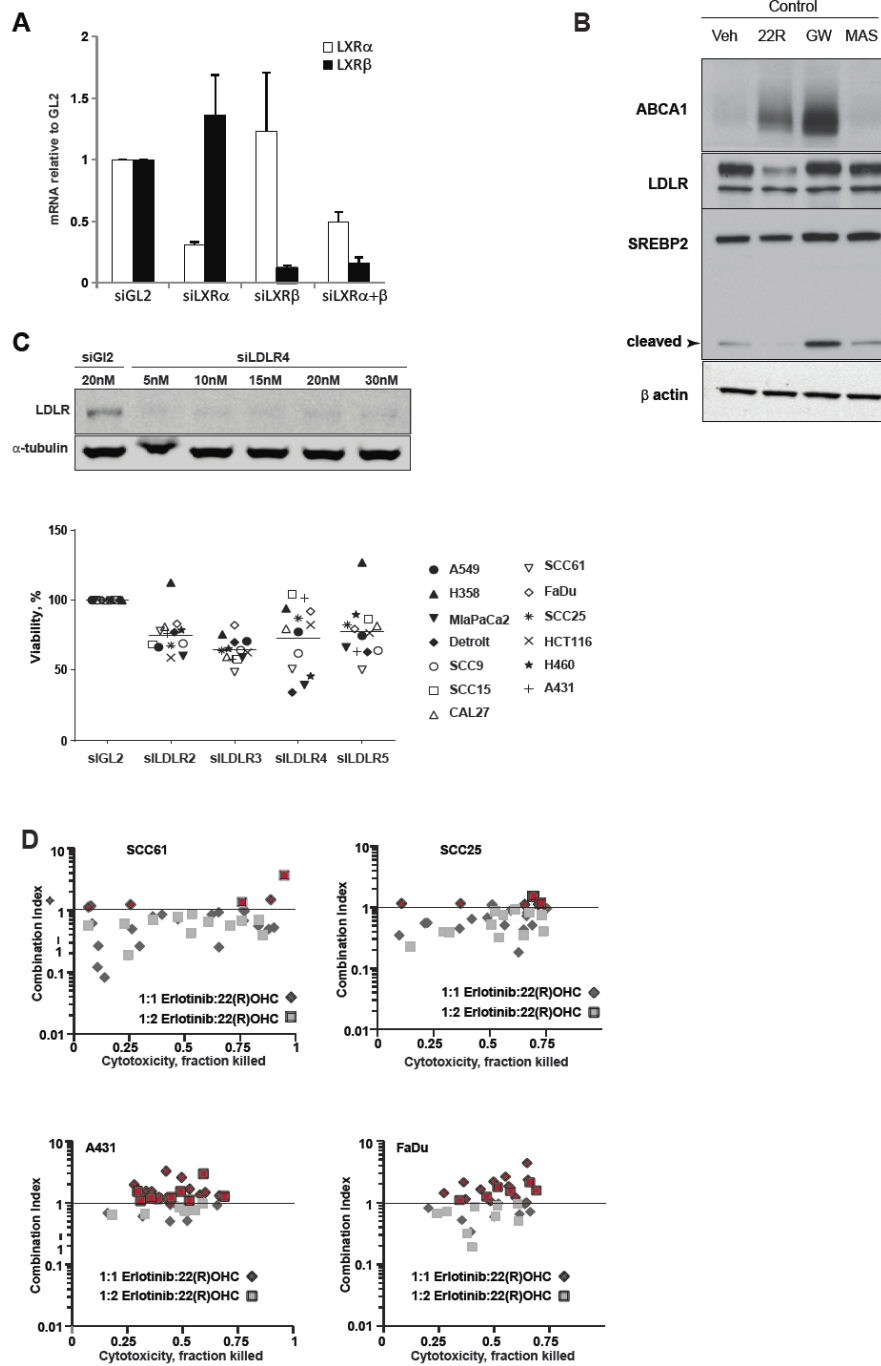
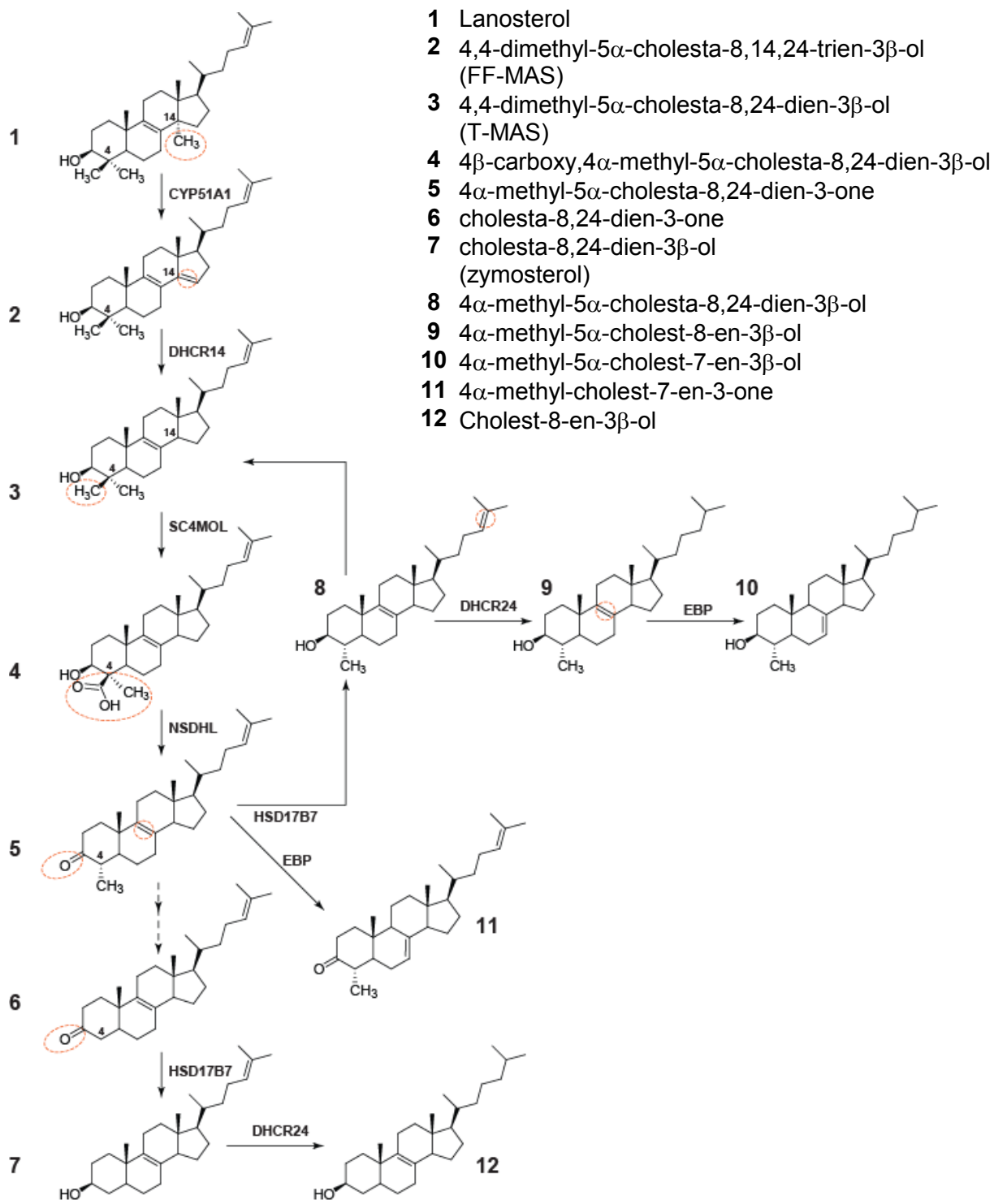


Figure S5. Effects of LDLR silencing and LXR agonists on cancer cell viability. **(A)** Selectivity of LXR silencing with siRNA. Shown are the averaged GL2-normalized results of LXR α and LXR β mRNA by qRT-PCR; *bars*, SEM. **(B)** Differential effect of LXR agonists in vitro. A431 cells were

treated with 1 μ M 22(R)-hydroxycholesterol, GW3965, or FF-MAS in 10% FBS-supplemented DMEM for 24 hours, and lysates were analyzed by Western blot. **(C)** LDLR silencing in SCC61 cells with siRNA depleted LDLR as determined by Western blot. Silencing of LDLR is cytotoxic in multiple PI3K and KRAS mutated carcinoma cell lines. Cells were transfected (HiPerFect, Qiagen) in triplicates with different LDLR siRNA (siLDLR2, siLDLR3, siLDLR4, siLDLR5) at 5 nmol/L. The viability was measured in 96 hours using CellTiter-Blue Viability Assay (Promega). **(D)** Testing 22(R)-hydroxycholesterol and erlotinib combinations in carcinoma cell lines shows synergistic-to-additive combinatorial effects. Shown are cytotoxicity vs. combination index (CI) plots.

Figure S6 related to Table 1. Cholesterol pathway metabolites from lanosterol to zymosterol and their corresponding enzymes. Metabolites numbered as in Table 1.



Supplemental Experimental Procedures.

Mouse strains. Tg(Krt5-Cre/ERT2)AJdg, 129S/Sv-Krastm4Tyj/J mice (original JAX stock 008180) and *Nsdhl*^{fix5}C57BL/6 congenic mice were kindly provided by Dr. Andres J.P. Klein-Szanto (Fox Chase Cancer Center, Philadelphia, PA), Dr. Rugang Zhang (The Wistar Institute, Philadelphia, PA) and Dr. Gail Herman (The Research Institute at Nationwide Children's Hospital and Department of Pediatrics, Columbus, OH) respectively. Tg(KRT14-cre)1Amc/J mice were purchased from the Jackson Laboratory (original JAX stock 004782).

Strain, genetic background	Source of mice	Gene	Ref.
Tg(Krt5-Cre/ERT2)AJdg FVB	Dr. John DiGiovanni	Tamoxifen responsive estrogen receptor ligand binding domain (ERT2) and Cre recombinase under the control of bovine Keratin 5 promoter	(Kataoka et al., 2008)
Tg(KRT14-cre)1Amc/J (C57BL/6xCBA)F1	JAX Mice: 004782	Constitutive Cre-mediated recombination system driven by the human keratin 14 (<i>KRT14</i>) promoter	(Raimondi et al., 2009)
<i>Nsdhl</i> ^{fix5} C57BL/6 congenic	Dr. Gail Herman	NSDHL ^{fix5} knockout allele that introduces LoxP sites flanking exon 5 of the gene	(Cunningham et al., 2015)
129S/Sv-Krastm4Tyj/J	JAX Mice: 008180	Knock-in transgene <i>LSL-Kras</i> ^{G12D}	(Jackson et al., 2001)

Genotyping. DNA was isolated by the standard Phenol/Chloroform/Isoamyl alcohol method. Mouse genotyping was performed by PCR using GoTaq Green Master Mix (M7122, Promega) according to the manufacturer's protocol with the following primers:

Nsdhl primers: forward primer (Frw), 5'-gtg cta ctg tag act gaa cc-3'; reverse primer (Rev): 5' gtg tcc ttg caa tct cag tg 3'. Primers produce a wild type band of 977 bp, a "floxed" *NSDHL*^{fix5} exon 5 band of 1106 bp and the Exon 5 deletion band of 271 bp.

Cre primers: oIMR1084, 5'-gcg gtc tgg cag taa aaa cta tc-3', oIMR1085, 5'-gtg aaa cag cat tgc tgt cac tt-3'; oIMR7338: 5'-cta ggc cac aga att gaa aga tct-3', oIMR7339, 5'-gta ggt gga aat tct

agc atc atc c-3'. Primers oIMR1084 + oIMR1085 produce the Cre transgenic band of 100 bp, and primers oIMR7338 + oIMR7339 will produce the internal control band of 325 bp.

LSL-KRas1 primers: forward1, 5'-gtc ttt ccc cag cac agt gc-3', forward2, 5'-agc tag cca cca tgg ctt gag taa gtc tgc a-3', reverse, 5'-ctc ttg cct acg cca cca gct c-3'. Primers produce a wild type band of 622 bp, and the LSL-cassette band of 500 bp. The recombined band is of 650 bp.

Sequences of siRNA.

siRNA name	Target sequence	Targeted mRNA	Product ID
GL2 Luciferase	CGTACGCGGAATACTTCGA	Non-targeting control	D-001100-01-20
SC4MOL_5	CACATCCTTTGGAGACTCTAA	NM_001017369, NM_006745	SI03159947
SC4MOL_6	CAGAACTAGTAGCTAACATT		SI03166457
SC4MOL_7	CTCTCAGTATAATGCCTATAA		SI03205398
SC4MOL_8	TTGAAGATACTTGGCACTATT		SI03243149
NSDHL_1	CAGCTTCATATTATACCGATT	NM_001129765, NM_015922	SI00661675
NSDHL_5	CTGTGGATTGATGAAATAACA		SI04151364
NSDHL_7	AGAGGATATGCTGTCAATGTA		SI04263329
CYP51A1_4	TCCGTTACAAACGAAGATCAA	NM_000786	SI00015610
CYP51A1_5	CTGATCGCTACTTACAGGATA		SI03093825
Hs_LDLR_2	TTACTCAAACCAGAGCCAC	NM_000527, NM_001195798, NM_001195799, NM_001195800, NM_001195802, NM_001195803	SI00011172
Hs_LDLR_3	TTCAAACCTCAGTTGGGTC		SI00011179
Hs_LDLR_4	AAGGACAAATCTGACGAGGAA		SI00011186
Hs_LDLR_5	CAACTACTATAGACAGGTT		SI03024525
Hs_NR1H3_2	CATGAATGAGCTGCAACTCAA	NM_001130101, NM_001130102, NM_001251934, NM_001251935, NM_005693	SI00080416
Hs_NR1H2_1	CCGGAAGAAGAAGATTCGGAA	NM_001256647, NM_007121	SI00094787

Supplemental references:

Cunningham, D., DeBarber, A.E., Bir, N., Binkley, L., Merkens, L.S., Steiner, R.D., and Herman, G.E. (2015). Analysis of hedgehog signaling in cerebellar granule cell precursors in a conditional *Nsdhl* allele demonstrates an essential role for cholesterol in postnatal CNS development. *Human molecular genetics* 24, 2808-2825.

Jackson, E.L., Willis, N., Mercer, K., Bronson, R.T., Crowley, D., Montoya, R., Jacks, T., and Tuveson, D.A. (2001). Analysis of lung tumor initiation and progression using conditional expression of oncogenic K-ras. *Genes & development* 15, 3243-3248.

Kataoka, K., Kim, D.J., Carbajal, S., Clifford, J.L., and DiGiovanni, J. (2008). Stage-specific disruption of Stat3 demonstrates a direct requirement during both the initiation and promotion stages of mouse skin tumorigenesis. *Carcinogenesis* 29, 1108-1114.

Liu, X.Y., Dangel, A.W., Kelley, R.I., Zhao, W., Denny, P., Botcherby, M., Cattanach, B., Peters, J., Hunsicker, P.R., Mallon, A.M., et al. (1999). The gene mutated in bare patches and striated mice encodes a novel 3beta-hydroxysteroid dehydrogenase. *Nature genetics* 22, 182-187.

Raimondi, A.R., Molinolo, A., and Gutkind, J.S. (2009). Rapamycin prevents early onset of tumorigenesis in an oral-specific K-ras and p53 two-hit carcinogenesis model. *Cancer research* 69, 4159-4166.